ACS APPLIED MATERIALS & INTERFACES

Research Article

www.acsami.org

Polydopamine Microcapsules with Different Wall Structures Prepared by a Template-Mediated Method for Enzyme Immobilization

Jiafu Shi, Chen Yang, Shaohua Zhang, Xiaoli Wang, Zhongyi Jiang,* Wenyan Zhang, Xiaokai Song, Qinghong Ai, and Chunyong Tian

Key Laboratory for Green Technology of Ministry of Education, School of Chemical Engineering and Technology, Tianjin University, Tianjin 300072, China

Supporting Information

ABSTRACT: Microcapsules with diverse wall structures may exhibit different performance in specific applications. In the present study, three kinds of mussel-inspired polydopamine (PDA) microcapsules with different wall structures have been prepared by a template-mediated method. More specifically, three types of $CaCO_3$ microspheres (*poly(allylamine hydrochloride), (PAH)-doped $CaCO_3$; pure-$CaCO_3$; and poly(styrene sulfonate sodium), (PSS)-doped $CaCO_3$*) were synthesized as sacrificial templates, which were then treated by dopamine to obtain the corresponding PDA-$CaCO_3$ microspheres. Through treating these microspheres with disodium ethylene diamine tetraacetic acid (EDTA-2Na) to remove $CaCO_3$, three types of PDA microcapsules were acquired: that was (1) PAH-PDA microcapsule with a thick (~600 nm) and highly porous capsule wall composed of interconnected networks, (2) pure-PDA microcapsule with a thick (~600 nm) and less porous capsule wall, (3) PSS-PDA microcapsule with a thin (~70 nm) and dense capsule wall. Several characterizations confirmed that a higher degree in porosity and interconnectivity of the capsule wall would lead to a higher mass transfer coefficient. When serving as the carrier for catalase (CAT) immobilization, these enzyme-encapsulated PDA microcapsules showed distinct structure-related activity and stability. In particular, PAH-PDA microcapsules with a wall of highly interconnected networks displayed several significant advantages, including increases in enzyme encapsulation efficiency and enzyme activity/stability and a decrease in enzyme leaching in comparison with other two types of PDA microcapsules. Besides, this hierarchically structured PAH-PDA microcapsule may find other promising applications in biocatalysis, biosensors, drug delivery, etc.

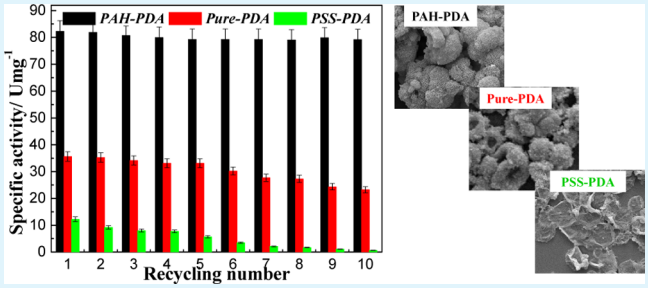

KEYWORDS: *polydopamine microcapsules, enzyme immobilization, hierarchical wall structure, template-mediated method*

1. INTRODUCTION

During the past decades, scientists have been dedicated to closed systems for encapsulation, protection, catalysis, and transportation, which are inspired by the structure and function of cells.[1−13] Among these, microcapsules have emerged as the important member of these systems due to their unique and hierarchical structures, which have been widely utilized as drug delivery vehicles, microreactors, and other encapsulants.[5,8,9,13] When applied in specific applications, controllable transfer or communication of substances between the outer environment and the microcapsules would be highly desired. More importantly, this transfer or communication is considered to be mainly dependent on the nano-/microstructure of the capsule wall (including the morphology, pore size, porosity, thickness, etc.).[14−18] For instance, Caruso and co-workers[14,15] have synthesized a series of microcapsules by using a layer-by-layer (LbL) assembly technique for drug delivery. The drug delivery performance or the intracellular degradation of the microcapsules can be facilely controlled through tailoring either the assembly number of polyelectrolytes or the cross-linking degree of the capsule wall. Wong and co-workers[17] have developed a nanoparticle/polymer tandem assembly for the synthesis of nanoparticle-assembled capsules. The thickness of the capsule wall can be conveniently changed by controlling the contacting time of the as-synthesized capsules with silicic acid, which can further influence the release property of the encapsulated cargoes. Ariga and co-workers[18] have also synthesized flake-shell capsules through the hydrothermal method. The acidic or basic treatment of the cargoes-loaded capsules can affect the compact structure of the flake wall, which then results in controlled release of the encapsulated cargoes from the silica capsules. Therefore, it can be concluded the nano-/microstructure of the capsule wall is worthy of extensive investigation. Especially, the relationship between the

Received: June 6, 2013
Accepted: September 23, 2013
Published: September 23, 2013

nano-/microstructure of the capsule wall and the application performance is urgently necessary to be explored for rational deign and synthesis of microcapsules.

In recent years, the bioadhesion of marine mussels has drawn intense interest. As a small molecular biomimetic adhesive, dopamine is particularly attractive due to the following aspects:[19−21] (1) universal and robust adhesion: forming strong covalent and noncovalent interactions with nearly all kinds of surfaces; (2) gentle and controllable self-polymerization: forming polydopamine (PDA) film, capsules, or other structures in near neutral pH value; (3) high biocompatibility and hydrophilicity. There is limited literature[22−27] relevant to the fabrication of PDA microcapsules for cargo (e.g., drug, enzyme, DNA, etc.) immobilization, and the synthesis of PDA comprising different wall structures has not been exploited.

Herein, three types of PDA microcapsules with different wall structures are synthesized through a template-mediated method for enzyme immobilization. More specifically, a series of $CaCO_3$ microspheres (*poly(styrene sulfonate sodium), (PSS)-doped $CaCO_3$; pure-$CaCO_3$; and poly(allylamine hydrochloride), (PAH)-doped $CaCO_3$*) are first synthesized as sacrificial templates, which are subsequently treated by dopamine to acquire PDA-$CaCO_3$ microspheres. The PDA microcapsules with different wall structures are obtained through treating the above microspheres with ethylene diamine tetraacetic acid (EDTA-2Na) to remove $CaCO_3$. The phys/chemical properties of the as-synthesized PDA microcapsules are characterized in detail. As an example, catalase (CAT) is chosen as a model enzyme for probing the relationship between the wall structure of the microcapsules and the catalytic activity of the encapsulated enzyme.

2. MATERIALS AND METHODS

2.1. Materials. Dopamine was purchased from Yuancheng Technology Development Co. Ltd. (Wuhan, China). Poly(sodium 4-styrenesulfonate) (PSS, M_W ca. 70 kDa), poly(allylamine hydrochloride) (PAH, M_W ca. 70 kDa), 2-amino-2-(hydroxymethyl)-1,3-propanediol (tris), catalase (CAT, hydrogen peroxide oxidoreductase; EC.1.11.1.6) from bovine liver, and fluorescein isothiocyanate (FITC) were purchased from Sigma-Aldrich Chemical Co. Calcium chloride ($CaCl_2$), sodium carbonate (Na_2CO_3), hydrochloric acid (HCl), sodium hydroxide (NaOH), disodium ethylene diamine tetraacetic acid (EDTA-2Na), disodium hydrogen phosphate (Na_2HPO_4), and sodium dihydrogen phosphate (NaH_2PO_4) of reagent grade quality were obtained from Guangfu (Tianjin, China). All other reagents were of analytical grade and used without further purification. Deionized water was used throughout all the experiments. The pH values of solutions were measured with a PHS-3C pH-meter (REX Instruments, PHS-3C, Shanghai, China) and adjusted by addition of HCl solution (100 mM) or NaOH solution (100 mM).

2.2. Preparation of Polydopamine (PDA) Microcapsules with Different Wall Structures. PAH-doped $CaCO_3$ microspheres with narrow size distribution (~5 μm in size) were used as sacrificial templates, which were prepared according to the coprecipitation method previously described in the literature.[28] Briefly, PAH (final concentration was 2 mg mL^{-1}) was completely dissolved in $CaCl_2$ solution (330 mM) in a beaker at 25 °C (room temperature). Then, an equal volume of Na_2CO_3 solution (330 mM) was rapidly added into the beaker under magnetic agitation and stirred continuously for 30 s. After settling without stirring for 3 min, the deposit was centrifuged and washed three times with deionized water. Finally, PAH-doped $CaCO_3$ particles with spherical shape about 5 μm in size were obtained. The particles (50 mg) were prewashed with tris-HCl buffer (50 mM, pH 8.5) via several centrifugation/redispersion cycles, which were then resuspended in tris-HCl buffer (10 mL, 50 mM, pH 8.5) with a concentration of 2 mg mL^{-1} of dopamine hydrochloride. The suspension was allowed to proceed for the allotted time with constant shaking. Next, the dark brown colored particles were centrifuged (3000*g*, 2 min) and washed with fresh tris-HCl buffer until the supernatant became colorless. The PAH-PDA microcapsules were obtained through removal of $CaCO_3$ in EDTA-2Na solution at 4 °C (15 mM).

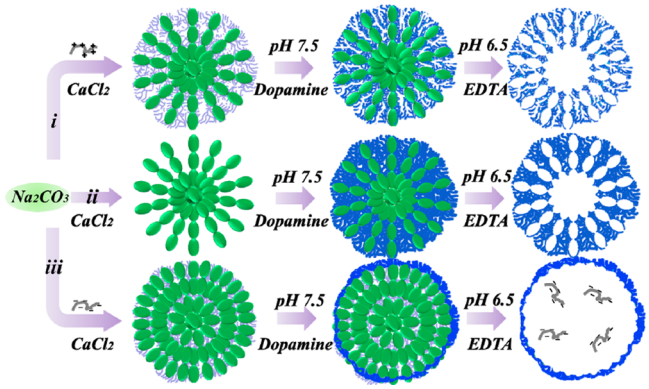

Figure 1. Schematic preparation of three PDA microcapsules (*i, PAH-PDA; ii, pure-PDA; and iii, PSS-PDA microcapsules*) with different wall structures.

The synthesis procedure and conditions of pure-PDA and PSS-PDA microcapsules were similar to those of PAH-PDA microcapsules. The only differences lay in the following aspects. For pure-PDA microcapsules, no additive was utilized during the synthesis of pure-$CaCO_3$ microspheres. For PSS-PDA microcapsules, PSS was utilized instead of PAH during the synthesis of PAH-$CaCO_3$ microspheres, and the settling time of the microspheres was fixed as 30 min instead of 3 min.

2.3. Mass Transfer Property. The mass transfer property of H_2O_2 from the bulk solution to the three PDA microcapsules was investigated according to the previous report.[29] An amount of 60 μL of concentrated microcapsule solution was immersed in 10 mL of a well-stirred pH 7.0, 30 mM tris-HCl buffer solution containing 19.4 mM H_2O_2 solutions. All the measurements were performed at 25 °C. At designed time intervals, the H_2O_2 concentration in the bulk solution was determined by a UV/vis spectrophotometer (Hitachi U-3010) as the detector. The fraction of H_2O_2 in solution was expressed as eq 1

$$\text{fraction of } H_2O_2 \text{ in solution } (\%) = \frac{C_t}{C_0} \times 100\% \quad (1)$$

where C_0 and C_t are the H_2O_2 concentrations in the bulk solution at time 0 and t, respectively (M).

According to previous reports,[30,31] the fraction of H_2O_2 in solution can be described by eq 2

$$\text{fraction of } H_2O_2 \text{ in solution } (\%) = \frac{\alpha}{1+\alpha}\left[1 + \sum_{n=1}^{\infty} \frac{6(1+\alpha)\exp(-D_m q_n^2/R^2)}{9 + 9\alpha + q_n^2\alpha^2}\right] \quad (2)$$

where D_m was the mass transfer coefficient of microcapsules (m^2 s^{-1}); R was the radius of a microcapsule (m); α was defined as $(V/N)(4\pi R^3/3)$; V was the volume of the solution excluding the space occupied by microcapsules (L); N was the number of microcapsules; and q_n was the nonzero positive roots of eq 3

$$\tan q_n - \frac{3q_n}{3 + \alpha q_n^2} = 0 \quad (3)$$

Upon the equations as described above, D_m could be obtained.

2.4. Characterizations. Scanning electron microscopy (SEM) images of the three types of microcapsules were recorded by using a

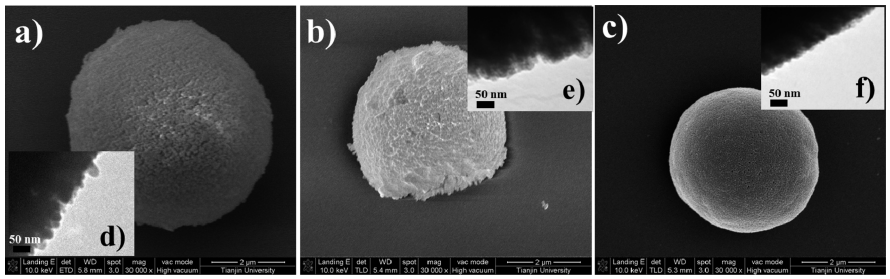

Figure 2. (a–c) SEM and (d–f) TEM images of (a, d) PAH-$CaCO_3$, (b, e) pure-$CaCO_3$, and (c, f) PSS-$CaCO_3$ microspheres.

field-emission SEM (FESEM, Nanosem 430). Transmission electron microscopy (TEM) observation was performed on a JEM-100CX II instrument. Fourier transform infrared (FTIR) spectra were obtained on a Nicolet-6700 spectrometer. 32 scans were accumulated with a resolution of 4 cm^{-1} for each spectrum. Optical images were taken using an Olympus BX51 microscope with a 100 × oil immersion objective lens (Olympus, Tokyo, Japan). Confocal laser scanning microscopy (CLSM) images were taken with a LSM 710 Confocal Microscope. The excitation wavelength was chosen as 488 nm according to the FITC-labeled enzymes.[24]

2.5. Assay of the Immobilized CAT. *2.5.1. Enzyme Immobilization.* A certain amount of CAT was dissolved in 1 mL of tris-HCl buffer solution (50 mM, pH 7.0). The enzyme solution was added into 4 mL of 330 mM $CaCl_2$ solution. The CAT-encapsulated PDA microcapsules were prepared following the same procedure as described above (section 2.2).

2.5.2. Enzyme Activity. The activity of immobilized CAT or free CAT was determined by direct measurement of the decrease in the absorbance of H_2O_2 at 240 nm due to enzymatic decomposition. Briefly, 30 μL of the immobilized CAT (or free CAT) (*approximately 0.0463 mg of enzyme*) was dispersed in 19.4 mM H_2O_2 in 10 mL of PBS (50 mM, pH 7.0) at 25 °C. After 5 min, the decrease in absorbance at 240 nm was recorded, and the activity was calculated. One unit (U) of CAT will decompose 1 μmol of H_2O_2 per minute at pH 7.0 and 25 °C.

2.5.3. Recycling and Storage Stability. The recycling stability of encapsulated CAT was determined by measuring the residual specific activity of CAT at 25 °C after it was used for several cycles. The CAT-encapsulated PDA microcapsules were collected by centrifugation after each reaction batch (25 °C, pH 7.0, reaction time 60 min), thoroughly rinsed with PBS, and reused in the next reaction cycle. During all the stability experiments, each result was obtained by averaging three individual experiments.

The storage stability of encapsulated CAT was determined by measuring the residual specific activity of CAT at 25 °C after it was stored with the gel state at 4 °C for a period of time.

2.5.4. Kinetic Parameters (K_m and V_{max}). K_m and V_{max} for the immobilized and free enzymes were determined using the Michaelis–Menten model, given by eq 4

$$\frac{1}{V} = \frac{K_m}{V_{max}} \times \frac{1}{[S]} + \frac{1}{V_{max}} \quad (4)$$

where V was the initial reaction rate (mM min^{-1}); [S] was the initial substrate concentration (mM); V_{max} was the maximum reaction rate attained at infinite initial substrate concentration (mM min^{-1}); and K_m was the Michaelis–Menten constant (mM). To determine the K_m and V_{max}, the activity assay was applied to different H_2O_2 concentrations from 3 to 35 mM. Enzyme activity was determined at 25 °C in PBS (50 mM, pH 7.0). Kinetic parameters for both the free and immobilized CAT were calculated accordingly.

3. RESULTS AND DISCUSSION

3.1. Synthesis and Characterizations of PDA Microcapsules with Different Wall Structures. *3.1.1. PAH-PDA Microcapsules.* Previous reports[28,32] have demonstrated that the addition of PAH, a cationic polymer, during the coprecipitation of $CaCl_2$ and Na_2CO_3 would result in PAH-segregated $CaCO_3$ microspheres comprising a porous structure. In our work, the spherical morphology of ca. 5 μm in size and porous near-surface structure of the PAH-$CaCO_3$ microspheres were acquired as shown in Figure 2a and 2d. Additionally, the FTIR spectrum of PAH-$CaCO_3$ microspheres had a distinct peak at ca. 1300 cm^{-1}, which was characteristic of C–N groups in PAH, indicating the successful entrapment of PAH within $CaCO_3$ microspheres. Meanwhile, a typical peak that was presented at 870 cm^{-1} was attributed to vaterite polymorphs of pure-$CaCO_3$.

After treating PAH-$CaCO_3$ microspheres with dopamine followed by EDTA-2Na etching, microcapsules with a thick and porous capsule wall composed of interconnected networks were obtained. The microstructures of the PAH-PDA microcapsules were characterized by SEM and TEM as shown in Figure 4. Specifically, the position of the arrows in Figure 4a revealed the successful formation of capsule structure with a wall thickness of ~600 nm (measured through SEM from Figure S1c, Supporting Information).[24] Figure 4b showed the microcapsule had a porous capsule wall with a unique interconnected macroporous network, which was then specifically characterized as shown in Figure 4c and 4d. The magnified SEM image in Figure 4c exhibited an interconnected 3D network of submicrometer-sized macropores in the capsule wall. Besides, some mesopores were also observed in the capsule wall (Figure 4c and 4d), which could form interconnected mass transfer channels. The formation of the hierarchical structures may be explained by the following aspects: dopamine diffused into the pores of PAH-$CaCO_3$ microspheres,[33] which was then polymerized into PDA and simultaneously reacted with amino groups of PAH,[34] thus forming a continuous layer attached to the inner pore surface (Figure 1*i*). After etching $CaCO_3$, the layered PDA-PAH complex was formed, which would then lead to a capsule wall composed of interconnected, layered networks.

3.1.2. Pure-PDA Microcapsules. Similar to PAH-$CaCO_3$ microparticles, the SEM image (Figure 2b) of pure-$CaCO_3$ microparticles also showed a spherical morphology with size of ca. 4 μm. A high-resolution TEM image (Figure 2e) illustrated that the near-surface region of pure-$CaCO_3$ microparticles had a porous structure, which could offer enough space for dopamine diffusion and polymerization. The chemical structure of the pure-$CaCO_3$ microsphere was also analyzed (Figure 3). A typical peak of 870 cm^{-1} was presented, which was attributed to vaterite polymorphs of pure-$CaCO_3$.

Accordingly, once pure-$CaCO_3$ microspheres were treated with dopamine followed by removing $CaCO_3$, pure-PDA microcapsules with a thick wall of ~600 nm (measured through optical microscopy from Figure S1b, Supporting

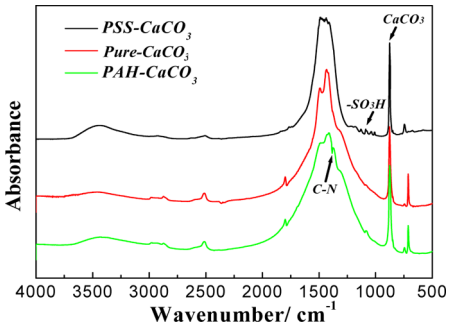

Figure 3. FTIR spectra of PAH-$CaCO_3$, pure-$CaCO_3$, and PSS-$CaCO_3$ microspheres.

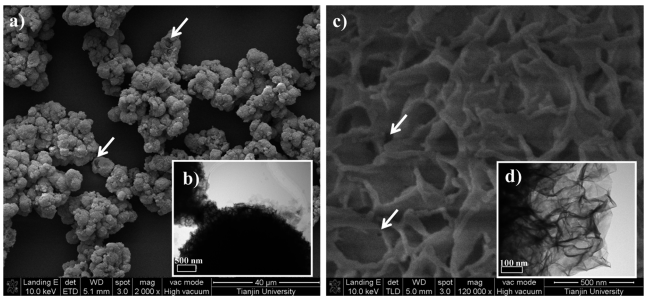

Figure 4. (a, c) SEM and (b, d) TEM images of PAH-PDA microcapsules.

Information)[35] could be acquired (Figure 5a). Moreover, as shown in Figure 5c, a less porous capsule wall was formed, which may be as a result of the replica of pure-$CaCO_3$ microspheres (Figure 1*ii*).[24,36]

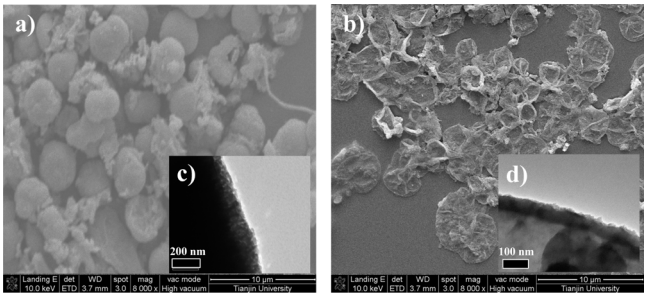

Figure 5. (a, b) SEM and (c, d) TEM images of (a, c) pure-PDA and (b, d) PSS-PDA microcapsules.

3.1.3. PSS-PDA Microcapsules. For contrast, PSS, as a typical anionic polyelectrolyte, was utilized as an additive during the synthesis of PDA microcapsules. In Figure 2c, a spherical microparticle with a size of ca. 4 μm was presented, and a dense surface structure could be found for PSS-$CaCO_3$ microspheres. Meanwhile, numerous closely aggregated nanoparticles were also shown in Figure 2f, which led to the nonporous near-surface structure of PSS-$CaCO_3$ microspheres. As shown in Figure 3, the FTIR spectrum of PSS-$CaCO_3$ microparticles proved the existence of vaterite polymorphs of $CaCO_3$ (870 cm^{-1}) and PSS components (1033 and 1190 cm^{-1}).

Subsequently, PSS-$CaCO_3$ microspheres were immersed in dopamine solution and subsequently treated with EDTA-2Na for the removal of $CaCO_3$. Microcapsules with a rather thin (~70 nm, measured through TEM from Figure S1a, Supporting Information)[3,37] and dense capsule wall were formed as shown in Figure 5b and 5d, mainly owing to the surface polymerization of dopamine and nearly no diffusion of dopamine into the template. (Figure 1*iii*)[23]

Besides, the chemical composition and corresponding discussion could be found in Figure S3 of the Supporting Information.

3.2. Mass Transfer Property of a Series of PDA Microcapsules. In most cases, enhancing the mass transfer rate of substance and the exposed active site number of microcapsules could greatly elevate their application performance. Therefore, mass transfer experiments were conducted by using H_2O_2 as a model molecule. The mass transfer coefficient of different PDA microcapsules was calculated and summarized in Figure 6. Obviously, the concentration of H_2O_2 quickly

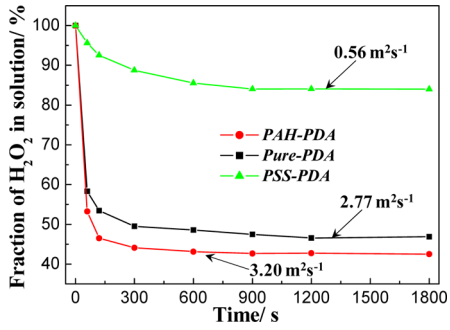

Figure 6. Mass transfer properties of PAH-PDA, pure-PDA, and PSS-PDA microcapsules.

decreased to a constant value within 300 s for PAH-PDA and pure-PDA microcapsules, indicating a relatively low mass transfer resistance. After calculation, the mass transfer coefficients of the above microcapsules were 3.20 and 2.77 $m^2\ s^{-1}$, respectively. In particular, the high mass transfer rate of PAH-PDA microcapsules was mainly attributed to the 3D interconnected capsule wall structure, which provided a multidimensional interconnected mesoporous and macroporous network for substance enrichment and low-resistance diffusion. In contrast, it would take nearly 900 s for the H_2O_2 concentration to decrease to a constant value for the PSS-PDA microcapsules, resulting in a rather low mass transfer coefficient of 0.56 $m^2\ s^{-1}$. This indicated that the PSS-PDA microcapsules possessed a much higher mass transfer resistance than the other two PDA microcapsules, which was in accordance with the differences in capsule wall structure of the microcapsules.

Large pore size and high porosity can facilitate the mass transfer of substrate(s)/product(s) through the capsule wall, which may also result in the leaching of larger molecules such as enzymes. The successful immobilization and leaching property of enzymes were thus explored in this study. Specifically, herein, CAT was first entrapped within $CaCO_3$ during the coprecipitation of $CaCl_2$ and Na_2CO_3. After dopamine treatment followed by EDTA-2Na etching, three CAT-encapsulated PDA microcapsules could be acquired. Furthermore, to verify the position of enzymes in/on the PDA microcapsules, FITC-labeled CAT was utilized during the synthesis of three PDA microcapsules, and the accurate location of enzymes in/on these microcapsules was determined by CLSM. As shown in Figure S2 (Supporting Information), the emitted fluorescence dots proved the successful encapsulation of CAT inside the microcapsules and the existence of the CAT

throughout the whole microcapsule from the wall to interior. Meanwhile, the highest fluorescence intensity for these three PDA microcapsules indicated that the majority of CAT was located in the interior of the hollow microcapsules. In addition, the fluorescence intensity from the near surface region of microcapsules was found to be slightly lower than that in the interior, suggesting that some CAT molecules were immobilized on the capsule wall. Collectively, enzymes were primarily physically encapsulated in the capsule lumen. Subsequently, the leakage of CAT from the capsule lumen was investigated as shown in Figure 7. In detail, CAT-encapsulated microcapsules

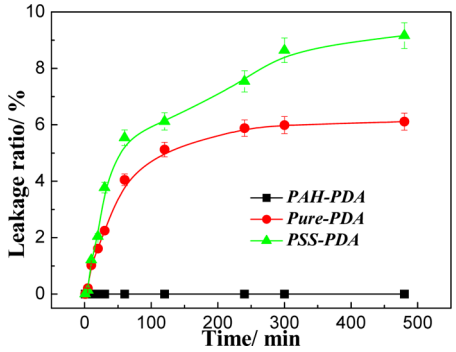

Figure 7. Leakage ratio of CAT encapsulated in PAH-PDA, pure-PDA, and PSS-PDA microcapsules.

were added into 3 mL of PBS (50 mM, pH 7.0) and incubated for a period of time at 25 °C. The mixture was then centrifuged, and the content of CAT in the supernatant was measured. The microcapsules were resuspended in 3 mL of fresh PBS (50 mM, pH = 7.0), and such a procedure was repeated seven times. The leakage of CAT was defined as the ratio of the cumulative leakage amount of CAT to the initial amount of encapsulated CAT. The PSS-PDA microcapsules leaked out ca. 9.0% CAT during the 480 min incubation due to the considerable rupture of the thin-wall microcapsules. As for pure-PDA microcapsules, the leakage ratio of ca. 6.0% was a little lower than that of PSS-PDA microcapsules. Then, the permeability of the PAH-PDA microcapsules was probed by CAT, and the leakage ratio of CAT decreased to a rather low value of nearly 0. This phenomenon should be ascribed to the following two reasons: (1) the strong electrostatic interaction between PAH and enzyme can prevent the leaching of enzymes from microcapsules and (2) the appropriate pore size in the capsule wall can also contribute to the retaining to enzyme in microcapsules.

3.3. Application of PDA Microcapsules for Enzyme Immobilization and Enzyme Catalysis. The enzyme encapsulation efficiency as a function of enzyme concentration for three PDA microcapsules was investigated in detail. More specifically, the enzyme encapsulation efficiency decreased monotonically with the increase of enzyme concentration from 0.1 to 2.0 mg mL^{-1}. Besides, PAH-PDA microcapsules exhibited the highest enzyme encapsulation efficiency at each CAT concentration. This may be due to the following reason: PAH, as a cationic polymer, can capture anionic enzymes to form a PAH−enzyme complex due to the electrostatic interaction. Then, it can be conjectured that the complex was easier to be entrapped within the $CaCO_3$ microspheres, which finally rendered enhanced enzyme encapsulation efficiency.

Accordingly, as shown in Figure 8, with the increase of enzyme concentration utilized during immobilization, each

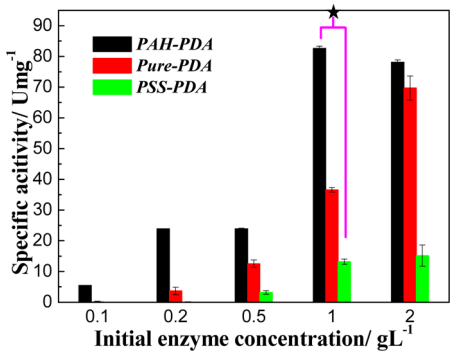

Figure 8. Specific activity of CAT encapsulated in PAH-PDA, pure-PDA, and PSS-PDA microcapsules as a function of initial enzyme concentration.

enzyme system exhibited an increased specific activity. This phenomenon was mainly owed to the increased enzyme encapsulation efficiency (or enzyme loading, Table 1). For each

Table 1. Encapsulation Efficiency for Different PDA Microcapsules

EE/%	0.1	0.2	0.5	1.0	2.0
PAH-PDA	95.2	89.4	84.6	65.2	33.4
pure-PDA	93.4	87.5	79.6	60.4	30.7
PSS-PDA	92.9	85.7	79.2	59.5	29.9

concentration, CAT encapsulated in PAH-PDA microcapsules showed the highest specific activity. Especially, at the concentration of 1.0 g L^{-1}, the specific activity of CAT encapsulated in PAH-PDA microcapsules reached a high value of ca. 83.85 U mg^{-1}, which was 2 and 6 times higher than that of CAT encapsulated in pure-PDA (36.58 U mg^{-1}) and PSS-PDA (13.17 U mg^{-1}) microcapsules, respectively. Such large differences in enzyme activity were ascribed to the differences in mass transfer property of the three PDA microcapsules. Specifically, PAH-PDA microcapsules possessed the lowest mass transfer resistance (Figure 6), leading to the highest reaction rate. Moreover, the Michaelis−Menten kinetics of the free and three enzyme systems were studied, and the corresponding Michaelis constant (K_m) and maximum reaction rate constant (V_{max}) were calculated from the Lineweaver−Burk plots (Table 2). The approximately equal value of K_m has

Table 2. Kinetic Parameters of Free and Immobilized Enzymes

	K_m (mM)	V_{max} (mM min^{-1})	V_{max}/K_m
free	25.70	13.46	0.52
PAH-PDA	26.06	13.29	0.51
pure-PDA	32.56	10.75	0.33
PSS-PDA	52.05	2.85	0.05

been observed from CAT-encapsulated PAH-PDA microcapsules in comparison with that observed from the free CAT, which was much higher than the other two microcapsules. Meanwhile, the ratio of V_{max}/K_m[38] for CAT encapsulated in PAH-PDA microcapsules was about twice and ten times higher than that observed from the CAT encapsulated in pure-PDA microcapsules and PSS-PDA microcapsules, respectively. Therefore, the affinity capacity between the enzyme and substrate has been enhanced, which

dx.doi.org/10.1021/am403523d | ACS Appl. Mater. Interfaces 2013, 5, 9991−9997

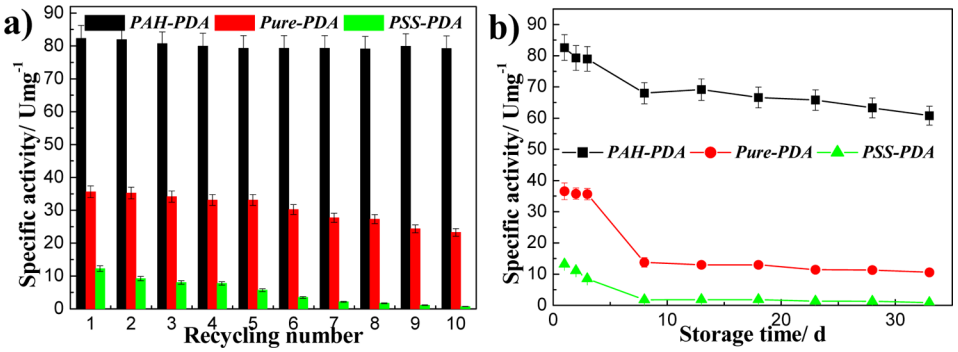

Figure 9. Specific activity of CAT immobilized in PAH-PDA (black), pure-PDA (red), and PSS-PDA (green), as a function of (a) recycling number and (b) storage time.

was to say PAH-PDA microcapsules can keep the immobilized enzyme in an active conformation and endow a more suitable microenvironment for enzymes.

For practical application, the structure stability for these three microcapsules during H_2O_2 degradation was quite essential. Therefore, after treating with H_2O_2, the morphologies of three PDA microcapsules were characterized by TEM and SEM as shown in Figure S4 (Supporting Information). Obviously, most of the CAT-encapsulated PSS-PDA microcapsules (Figure S4a, Supporting Information) were broken after several cycles' reaction. By contrast (Figure S4b and S4c, Supporting Information), the other two CAT-encapsulated microcapsules (pure-PDA and PAH-PDA microcapsules) well retained their initial morphology or structure. To corroborate the structure−performance relationship, the recycling stabilities of the immobilized CAT were determined for 10 successive batch reactions at 25 °C for 120 min as shown in Figure 9a. After 10 times recycling, the activity of CAT encapsulated in PAH-PDA microcapsules was nearly unaltered, remaining a specific activity of ca. 80.00 U mg^{-1} owing to its robust nature and high porosity. In contrast, the specific activity of CAT encapsulated in PSS-PDA microcapsules decreased from 12.26 U mg^{-1} to a rather low value of 0.66 U mg^{-1} after 10 times recycling. This may be ascribed to the vigorous agitation causing the breaking of microcapsules, which finally led to the leaching of enzyme and decrease in enzyme activity. Besides, the operational stability of CAT encapsulated in pure-PDA microcapsules was nearly half as low as that of CAT encapsulated in PAH-PDA microcapsules but much higher than that of PSS-PDA microcapsules due to its robust mechanical stability.

Finally, the storage stabilities for three CAT-encapsulated microcapsules were investigated as illustrated in Figure 9b. After storing for 33 days, CAT encapsulated in PAH-PDA microcapsules can effectively maintain enzyme activity with a specific activity of 60.78 U mg^{-1} (initial specific activity: 82.62 U mg^{-1}), while CAT encapsulated in pure-PDA microcapsules can only acquire a specific activity of 10.55 U mg^{-1} (initial specific activity: 36.58 U mg^{-1}). This result indicated that PAH-PDA microcapsules provided an appropriate environment for enzyme molecules. Even worse was that CAT encapsulated in PDA microcapsules retained almost no activity after storing for 30 days.

4. CONCLUSIONS

In summary, we have synthesized three PDA microcapsules with different wall structures through a template-mediated method. Specifically, by using PAH-doped $CaCO_3$ microspheres as templates, the PAH-PDA microcapsule with a thick and highly porous capsule wall composed of highly interconnected networks can be obtained; by using pure-$CaCO_3$ microspheres as templates, pure-PDA microcapsules with a thick and less porous capsule wall can be obtained; and by using PSS-doped $CaCO_3$ microspheres as templates, PSS-PDA microcapsule with a thin and dense capsule wall can be obtained. When utilized for enzyme immobilization, three CAT-encapsulated PDA microcapsules exhibited distinct structure-related activity and stability. Specifically, a higher degree in porosity and interconnectivity of the capsule wall would lead to a higher mass transfer coefficient, rendering higher enzymatic activity (PAH-PDA microcapsule, 83.85 U mg^{-1}; pure-PDA microcapsule, 36.58 U mg^{-1}; and PSS-PDA microcapsule, 13.17 U mg^{-1}). In addition, due to the unique chemical and structural composition of PAH-PDA microcapsules, CAT encapsulated in such a microcapsule won a suitable microenvironment, leading to an enhanced recycling and storage stability in comparison to the other two PDA (pure-PDA and PSS-PDA) microcapsules. This rationally integrated architecture may find a broad range of applications in biocatalysis, biosensing, drug delivery, and so on.

■ ASSOCIATED CONTENT

Ⓢ Supporting Information

TEM image of PSS-PDA microcapsules, optical microscopy image of pure-PDA microcapsules, and SEM image of PAH-PDA microcapsules; CLSM images of PSS-PDA, pure-PDA, and PAH-PDA microcapsules; FTIR spectra of PAH-PDA, pure-PDA, and PSS-PDA microcapsules; TEM and SEM images of PSS-PDA, pure-PDA, and PAH-PDA microcapsules after treating them with H_2O_2; and FTIR spectra of three typical microcapsules before and after treating them with H_2O_2. This material is available free of charge via the Internet at http://pubs.acs.org.

■ AUTHOR INFORMATION

Corresponding Author

*E-mail: zhyjiang@tju.edu.cn. Tel.: +86-022-27406646. Fax: +86-022-27406646.

Notes

The authors declare no competing financial interest.

■ ACKNOWLEDGMENTS

The authors thank the financial support from the National Basic Research Program of China (2009CB724705), National

Science Fund for Distinguished Young Scholars (21125627), and the Program of Introducing Talents of Discipline to Universities (B06006).

REFERENCES

(1) Oberholzer, T.; Nierhaus, K. H.; Luisi, P. L. *Biochem. Biophys. Res. Commun.* **1999**, *261*, 238−241.
(2) van Dongen, S. F. M.; de Hoog, H. P. M.; Peters, R.; Nallani, M.; Nolte, R. J. M.; van Hest, J. C. M. *Chem. Rev.* **2009**, *109*, 6212−6274.
(3) Yang, S. H.; Kang, S. M.; Lee, K. B.; Chung, T. D.; Lee, H.; Choi, I. S. *J. Am. Chem. Soc.* **2011**, *133*, 2795−2797.
(4) Fakhrullin, R. F.; Minullina, R. T. *Langmuir* **2009**, *25*, 6617−6621.
(5) Tong, W. J.; Song, X. X.; Gao, C. Y. *Chem. Soc. Rev.* **2012**, *41*, 6103−6124.
(6) Brinkhuis, R. P.; Rutjes, F.; van Hest, J. C. M. *Polym. Chem.* **2011**, *2*, 1449−1462.
(7) He, Q.; Cui, Y.; Li, J. B. *Chem. Soc. Rev.* **2009**, *38*, 2292−2303.
(8) Lensen, D.; Vriezema, D. M.; van Hest, J. C. M. *Macromol. Biosci.* **2008**, *8*, 991−1005.
(9) De Cock, L. J.; De Koker, S.; De Geest, B. G.; Grooten, J.; Vervaet, C.; Remon, J. P.; Sukhorukov, G. B.; Antipina, M. N. *Angew. Chem., Int. Ed.* **2010**, *49*, 6954−6973.
(10) Sukhorukov, G. B.; Mohwald, H. *Trends Biotechnol.* **2007**, *25*, 93−98.
(11) Wang, Y.; Angelatos, A. S.; Caruso, F. *Chem. Mater.* **2008**, *20*, 848−858.
(12) De Geest, B. G.; Sanders, N. N.; Sukhorukov, G. B.; Demeester, J.; De Smedt, S. C. *Chem. Soc. Rev.* **2007**, *36*, 636−649.
(13) Vriezema, D. M.; Comellas Aragones, M.; Elemans, J.; Cornelissen, J.; Rowan, A. E.; Nolte, R. J. *Chem. Rev.* **2005**, *105*, 1445−1490.
(14) Liang, K.; Such, G. K.; Zhu, Z. Y.; Dodds, S. J.; Johnston, A. P. R.; Cui, J. W.; Ejima, H.; Caruso, F. *ACS Nano* **2012**, *6*, 10186−10194.
(15) Kinnane, C. R.; Such, G. K.; Caruso, F. *Macromolecules* **2011**, *44*, 1194−1202.
(16) Wang, Y.; Angelatos, A. S.; Caruso, F. *Chem. Mater.* **2008**, *20*, 848−858.
(17) Bagaria, H. G.; Kadali, S. B.; Wong, M. S. *Chem. Mater.* **2011**, *23*, 301−308.
(18) Ji, Q. M.; Guo, C. Y.; Yu, X. Y.; Ochs, C. J.; Hill, J. P.; Caruso, F.; Nakazawa, H.; Ariga, K. *Small* **2012**, *8*, 2345−2349.
(19) Zhang, L.; Wu, J. J.; Wang, Y. X.; Long, Y. H.; Zhao, N.; Xu, J. *J. Am. Chem. Soc.* **2012**, *134*, 9879−9881.
(20) Lee, H.; Dellatore, S. M.; Miller, W. M.; Messersmith, P. B. *Science* **2007**, *318*, 426−430.
(21) Lee, B. P.; Messersmith, P. B.; Israelachvili, J. N.; Waite, J. H. *Annu. Rev. Mater. Res.* **2011**, *41*, 99−132.
(22) Zhang, L.; Shi, J. F.; Jiang, Z. Y.; Jiang, Y. J.; Meng, R. J.; Zhu, Y. Y.; Liang, Y. P.; Zheng, Y. *ACS Appl. Mater. Interfaces* **2011**, *3*, 597−605.
(23) Sedó, J.; Saiz-Poseu, J.; Busqué, F.; Ruiz-Molina1, D. *Adv. Mater.* **2013**, *25*, 653−701.
(24) Zhang, L.; Shi, J. F.; Jiang, Z. Y.; Jiang, Y. J.; Qiao, S. Z.; Li, J. A.; Wang, R.; Meng, R. J.; Zhu, Y. Y.; Zheng, Y. *Green Chem.* **2011**, *13*, 300−306.
(25) Cui, J. W.; Wang, Y. J.; Postma, A.; Hao, J. C.; Hosta-Rigau, L.; Caruso, F. *Adv. Funct. Mater.* **2010**, *20*, 1625−1631.
(26) Cui, J. W.; Yan, Y.; Such, G. K.; Liang, K.; Ochs, C. J.; Postma, A.; Caruso, F. *Biomacromolecules* **2012**, *13*, 2225−2228.
(27) Aviles, M. O.; Lin, C. H.; Zelivyanskaya, M.; Graham, J. G.; Boehler, R. M.; Messersmith, P. B.; Shea, L. D. *Biomaterials* **2010**, *31*, 1140−1147.
(28) Wang, Z. P.; Mohwald, H.; Gao, C. Y. *Langmuir* **2011**, *27*, 1286−1291.
(29) Zhang, Y. F.; Wu, H.; Li, J.; Li, L.; Jiang, Y. J.; Jiang, Z. Y. *Chem. Mater.* **2008**, *20*, 1041−1048.
(30) Coradin, T.; Mercey, E.; Lisnard, L.; Livage, J. *Chem. Commun.* **2001**, 2496−2497.
(31) Zhang, L. Y.; Yao, S. J.; Guan, Y. X. *J. Chem. Eng. Data* **2003**, *48*, 864−868.
(32) Wang, Z. P.; Mohwald, H.; Gao, C. Y. *ACS Nano* **2011**, *5*, 3930−3936.
(33) Shi, J. F.; Zhang, W. Y.; Wang, X. L.; Jiang, Z. Y.; Zhang, S. H.; Zhang, X. M.; Zhang, C. H.; Song, X. K.; Ai, Q. H. *ACS Appl. Mater. Interfaces* **2013**, *5*, 5174−5185.
(34) Kang, S. M.; Hwang, N. S.; Yeom, J.; Park, S. Y.; Messersmith, P. B.; Choi, I. S.; Langer, R.; Anderson, D. G.; Lee, H. *Adv. Funct. Mater.* **2012**, *22*, 2949−2955.
(35) Postma, A.; Yan, Y.; Wang, Y. J.; Zelikin, A. N.; Tjipto, E.; Caruso, F. *Chem. Mater.* **2009**, *21*, 3042−3044.
(36) Zheng, Y.; Zhang, L.; Shi, J. F.; Liang, Y. P.; Wang, X. L.; Jiang, Z. Y. *Microporous Mesoporous Mater.* **2012**, *152*, 122−127.
(37) Saiz-Poseu, J.; Sedó, J.; García, B.; Benaiges, C.; Parella, T.; Alibés, R.; Hernando, J.; Busqué, F.; Ruiz-Molina, D. *Adv. Mater.* **2013**, *25*, 2066−2070.
(38) Chen, L.; Wei, B.; Zhang, X.; Li, C. *Small* **2013**, *9*, 2331−2340.